

UNCLASSIFIED

Defense Technical Information Center
Compilation Part Notice

ADP013094

TITLE: Current Instabilities in Negative Differential Resistance Region of a Large Area Resonant Tunneling Diode

DISTRIBUTION: Approved for public release, distribution unlimited
Availability: Hard copy only.

This paper is part of the following report:

TITLE: Nanostructures: Physics and Technology International Symposium [8th] Held in St. Petersburg, Russia on June 19-23, 2000 Proceedings

To order the complete compilation report, use: ADA407315

The component part is provided here to allow users access to individually authored sections of proceedings, annals, symposia, etc. However, the component should be considered within the context of the overall compilation report and not as a stand-alone technical report.

The following component part numbers comprise the compilation report:

ADP013002 thru ADP013146

UNCLASSIFIED

Current instabilities in negative differential resistance region of a large area resonant tunneling diode

V. G. Popov, Yu. V. Dubrovskii, K. L. Wang[†], L. Eaves[‡] and J. C. Maan[§]

Institute of Microelectronics Technology RAS,
142432, Chernogolovka, Moscow District, Russia

[†] Electrical Engineering Department, University of California, Los-Angeles, USA

[‡] University of Nottingham, NG72 RD Nottingham, United Kingdom

[§] University of Nijmegen, 6525ED Nijmegen, The Netherlands

Abstract. The current instabilities in the negative differential conductance region of the resonance tunneling diode have been thoroughly studied at different parameters of the external circuit. The instabilities were dealt with an excitement of the current oscillations in the circuit. In a homogeneous approximation two small signal equivalent circuits of the resonant tunneling diode were used to describe the observed instabilities. Some revealed effects were out of the approximation.

Inhomogeneous current instabilities in the semiconductor devices are of the most interest investigated already 50 years. They were observed in a wide range of the devices [1]. As far as we know, a resonant tunneling diode (RTD) has not been experimentally investigated for the inhomogeneous current instabilities yet. Some theoretical works already predict this kind of instabilities in the RTD [2–6]. For RTD local probe method could not be lucky, in spite that it was successfully used to study the inhomogeneous instability previously [7]. Another way to study RTD for the instabilities is a comparison of the experimental data with calculated ones from widely used RTD models derived in the preposition of a homogeneous lateral current distribution along the tunnel junction [8, 9], and search for features which could not be explained by these models. For comparison with calculations we have measured R_T — the threshold negative differential resistance (NDR), i.e. the R_T values at which the current instabilities in the measuring circuit arisen.

The investigated resonant tunneling diodes were fabricated from InGaAs-AlAs heterostructure. Mesa structures had 70 μm in diameter and was made by conventional wet etching.

The simplified measurement circuit is shown in Fig. 1(a). The typical current-voltage characteristics of the diodes at room temperatures is shown in Fig. 2(a). The NDR was observed in the voltage range from 0.47 V to 1 V when the diode was shunted with resistance $R_S = 25 \Omega$ and the inductance of the shunt was very low approximately 10 nHn (curve 1 in Fig. 2(a)). To obtain actual I–V curves the current through the shunt was subtracted in situ by means of balance scheme. One can see current steps and jumps on the I–V curves (curve 2, Fig. 2(a)) measured without shunt resistance, but with $C_S = 15 \text{ pF}$ capacity shunt, and $R_L = 47 \Omega$, $L_L = 100 \text{ mHn}$ (see Fig. 1(a)). The current steps and jumps are just the manifestations of the current instabilities in the circuit. High frequency oscillations (up to 1 GHz) were observed in the voltage range of the current steps and they were absent out of the range. One can see the NDR region without instabilities at bias voltages between points A and B in Fig. 2(a), curve 2. The current oscillations arisen in the point A,

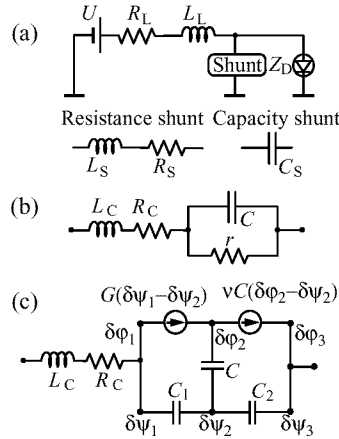


Fig. 1. (a) The measuring circuit with RTD. R_L, L_L are load resistance and inductance, U is sweep generator. (b) RC — model of the RTD. R_C is contact resistance, L_C is bonding inductance, r is differential resistance of the tunnel junction, C is differential capacity. (c) The ST — model of the RTD. $\delta\phi_i$ — electrochemical potential variations of the emitter ($i = 1$), well ($i = 2$), collector ($i = 3$). $\delta\psi_i$ — electrical potential variations of the emitter ($i = 1$), well ($i = 2$), collector ($i = 3$). G — emitter-well transconductance, C_1, C_2, C — emitter, collector barriers and well capacitancies.

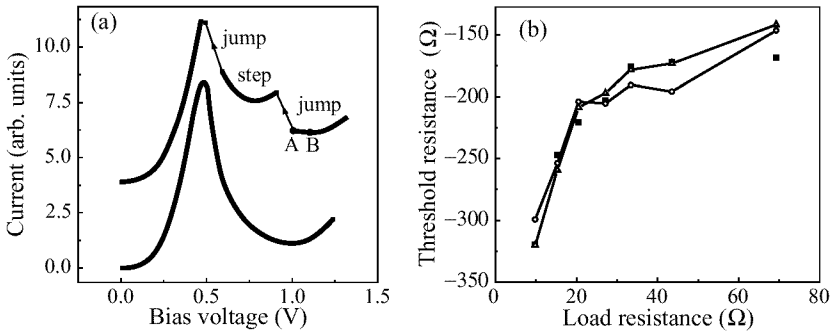


Fig. 2. (a) The I–V characteristics of the RTD. Curve 1 is I–V curve measured for the diode shunting with the $R_S = 25 \Omega$ and $L_S \approx 10$ nHn. Curve 2 is I–V curve measured for the diode shunting with the $C_S = 15$ pF. The threshold resistance R_T is the NDR measured at point A. (b) The R_T dependence upon the load resistance R_L . Square symbols are the experimental data. Triangle and circles symbols are calculated values for RC and ST models of the RTD.

when the bias voltage decreased. Thus measuring the NDR value in the point A we get the threshold resistance R_T . In the theoretical models R_T can be related to the measuring circuit parameters and internal parameters of the diode. The dependencies of R_T on the different parameters of the measuring circuit were obtained experimentally and then compared with calculated ones.

Figure 2(b) shows the dependence of the threshold resistance R_T on the R_L — load resistance. Other circuit parameters were fixed. Figure 3(a) shows the dependence of the threshold resistance R_T on the R_S — shunt resistance, with $R_L = 9.8 \Omega$, and $L_L = 10$ mHn kept constant, in this measurements we did not add any shunt capacitance. Figure 3(b) shows the dependence of the threshold resistance R_T on the C_S — shunt capacitance, with

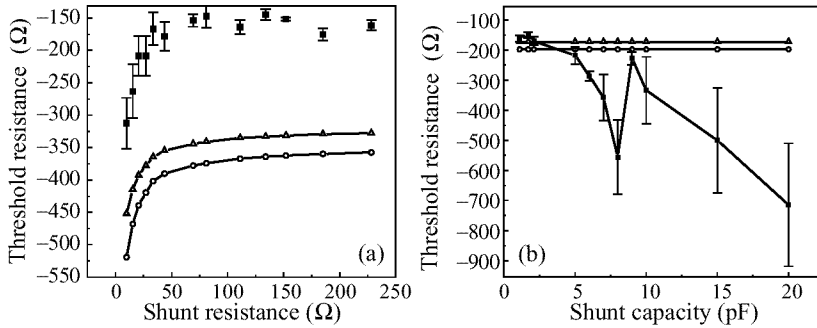


Fig. 3. (a) The R_T dependence upon the shunt resistance R_L . Square symbols are the experimental data. Triangle and circles symbols are calculated values for RC and ST models of the RTD. (b) The R_T dependence on the shunt capacity C_S . Square symbols are the experimental data. Triangle and circles symbols are calculated values for RC and ST models of the RTD.

fixed $R_L = 47 \Omega$, and $L_L = 10 \text{ mHn}$, shunt resistance was absent. In all the figures the experimental data are presented by square symbols. To calculate theoretical values of the threshold resistance for different circuit parameters it is necessary to know equivalent RTD circuit which definitely include NDR. Than knowing the full equivalent circuit we found the boundary between circuit stable and unstable conditions. From the boundary conditions relations between R_T other circuits parameters can be found. The equivalent RTD circuit depends on the model used to describe the resonant tunneling diode. We used two equivalent circuits: the first one — RC model (Fig. 1(b)) — is suitable for coherent tunneling [8], and the second one — ST model (Fig. 1(c)) — for sequential tunneling processes [9]. It is necessary to emphasize here, once more, that both equivalent circuits described the uniform distribution of the current along the tunneling structure.

The calculated data are shown in Figs. 2(b)–3(b) by triangles for RC model, and by circles for ST model. The procedure of comparison was following. First of all from comparison of R_T dependencies on R_L (Fig. 2(b)) we obtain best fit parameters for R_C , L_C and C for RC model and R_C , L_C , C_1 , C_2 , ν for ST model. With found best fit parameters theoretical dependence of R_T on R_S was drawn in Fig. 3(a). The R_T experimental and theoretical values differ two times. If the best fit was done for data in Fig. 3(a), than the strong discrepancies appeared for R_T on R_L and R_S dependencies. In other words it was impossible to make best fit for R_T on R_L and R_S dependencies at the same time. More drastic discrepancies was found for R_T on C_S data (see Fig. 3(b)). For both model in the range of used C_S value the dependence should be constant. The experiment shows quite complicated dependence with clear local minimum around $C_S = 7 \text{ pF}$. The experiment has demonstrated that the current instabilities of the RTD with 20 nF internal capacity are very sensitive to change of $\Delta C_S \sim 1 \text{ pF}$. Moreover a frequency of the current oscillations is about 250 MHz that is higher than the cut-off frequency of the diode ($\sim 10 \text{ MHz}$) calculated for both models. It worth to note that the models have been tested with ultra-high frequency techniques on the diode with quite small lateral sizes ($\sim 20\text{--}30 \mu\text{m}$) [8, 9] and relatively large negative differential resistance. We used the diode that had larger lateral sizes than in previous studies. From the comparison of the experimental and calculated data we concluded that current models based on the uniform distribution of the tunneling current along the junction can not explain experimental findings. The theories where inhomogeneous distribution of the current along the junction was considered did not propose any equivalent circuit which in principle would permit one

to make the similar comparison with experimental data. It means that more sophisticated approaches are necessary to develop for proving these theories.

Acknowledgements

This work was partly supported by INTAS (97-11475), National programs “Physics of solid state nanostructures” (grants 97-1057), “Physics of quantum and wave processes” (V.3), “Surface atomic structure” (3.11.99), and RFBR (98-02-17642).

References

- [1] M. P. Shaw, V. V. Mitin, E. Schöll and H. L. Grubin, *The Physics of Instabilities in Solid State Electron Devices* (New York, Plenum Press), 1992.
- [2] A. Wacker and E. Schöll, *J. Appl. Phys.* **78**, 1 (1995).
- [3] M. Meixner, P. Rodin, E. Schöll and A. Wacker, *Eur. Phys. J. B* (in print), (1999).
- [4] M. N. Feiginov, S. A. Mikhailov and V. A. Volkov, *Phys. Low-Dim. Struct.* **9**, 1 (1994).
- [5] M. N. Feiginov and V. A. Volkov, *Abstracts of the 24th Int. Conf. on the Physics of Semiconductors* **9**, 1 (1994).
- [6] M. N. Feiginov and V. A. Volkov, *Pis'ma ZheTF* **68**, 633 (1998).
- [7] J. B. Gunn, *Plasma Effects in Solids* (Paris 1964), 199 (1964).
- [8] T. Wei, S. Stapleton and E. Berolo, *J. Appl. Phys.* **73**, 829 (1993).
- [9] J. P. Mattia, A. L. McWhorter, R. J. Aggarwal, F. Rana, E. R. Brown and P. Maki, *J. Appl. Phys.* **84**, 1140 (1998).